Ultrafast extreme-ultraviolet ARPES studies of electronic dynamics in two-dimensional materials

Jan Heye Buss[a], Julian Maklar[a], Frédéric Joucken[a], He Wang[a], Yiming Xu[a], Sung-Kwan Mo[b], Alessandra Lanzara[a,c], and Robert A. Kaindl[a]
[a]Materials Sciences Division, E. O. Lawrence Berkeley National Laboratory, Berkeley, CA, USA
[b]Advanced Light Source, E. O. Lawrence Berkeley National Laboratory, Berkeley, CA, USA
[c]Department of Physics, University of California at Berkeley, Berkeley, CA, USA

ABSTRACT

The intriguing electronic properties of two-dimensional materials motivates experiments to resolve their rapid, microscopic interactions and dynamics across momentum space. Essential insight into the electronic momentum-space dynamics can be obtained directly via time- and angle-resolved photoemission spectroscopy (trARPES). We discuss the development of a high-repetition rate trARPES setup that employs a bright source of narrowband, extreme-UV harmonics around 22.3 eV, and its application to sensitive studies of materials dynamics. In the bulk transition-metal dichalcogenide $MoSe_2$ momentum-space quasiparticle scattering is observed after resonant excitation at the *K*-point exciton line, resulting in the time-delayed buildup of electrons at the Σ-point conduction band minimum. We will discuss this and other aspects of the non-equilibrium electronic response accessible with the extreme-UV trARPES probe.

Keywords: Time- and angle-resolved photoemission spectroscopy, Ultrafast phenomena in semiconductors, Transition-metal dichalcogenides, Molybdenum Diselenide

1. INTRODUCTION

Time- and angle-resolved photoemission spectroscopy (trARPES) is an important contemporary technique that provides access to both transient changes of the electronic band structure as well as to non-equilibrium quasiparticle distributions in energy and momentum space. In recent years, this method has evolved rapidly and enabled unprecedented insight into quantum materials, including e.g. studies of quasiparticle and gap dynamics in high-transition temperature superconductors [1, 2], investigations of quenching dynamics of charge-density-waves [3], the sensitive mapping of the unoccupied band structure via non-equilibrium carriers [4], and the first observation of light-driven Floquet-states in a topological insulator [5]. Since the in-plane momenta of the photoemitted electrons are conserved in ARPES, this method and its time-resolved version are thus predestined to study the band structures and quasiparticle dynamics of two-dimensional and layered materials such as transition-metal dichalcogenides (TMDCs). Semiconducting TMDCs exhibit fascinating physical properties, including e.g. large spin-orbit splitting and strongly Coulomb-bound electron-hole pairs [6, 7]. Their electronic bands transform from an indirect to a direct band-gap semiconductor when reaching the monolayer limit, yielding strong photoluminescence and providing unique optical access to the spin- and valley degrees-of-freedom. Such properties render TMDCs of significant interest for future applications in nanoscale and high-speed electronics [8, 9]. This motivates trARPES studies for direct insight into the non-equilibrium dynamics and interactions of carriers and Coulomb-bound electron-hole pairs in TMDCs.

In the following, we discuss the development of a powerful setup for trARPES based on a bright source of narrowband, extreme-UV (XUV) pulses around 22.3 eV operating at 50-kHz repetition rate [10], along with its initial application to ultrafast investigations of layered transition-metal dichalcogenides. In semiconducting $MoSe_2$ this allows for studies of the electronic dynamics across the full Brillouin zone with high sensitivity, yielding insights into the indirect band gap as well as fast momentum transfer of the photo-excited quasiparticles.

2. EXTREME-UV ULTRAFAST PHOTOEMISSION AT HIGH REPETITION RATES

Our trARPES setup is based on the development of a bright source of XUV femtosecond pulses around 22.3 eV [10]. Efficient table-top conversion of ultrafast pulses into the XUV generally relies on high-harmonic generation (HHG),

Ultrafast Phenomena and Nanophotonics XXI, edited by Markus Betz, Abdulhakem Y. Elezzabi,
Proc. of SPIE Vol. 10102, 101020I · © 2017 SPIE · CCC code: 0277-786X/17/$18
doi: 10.1117/12.2251249

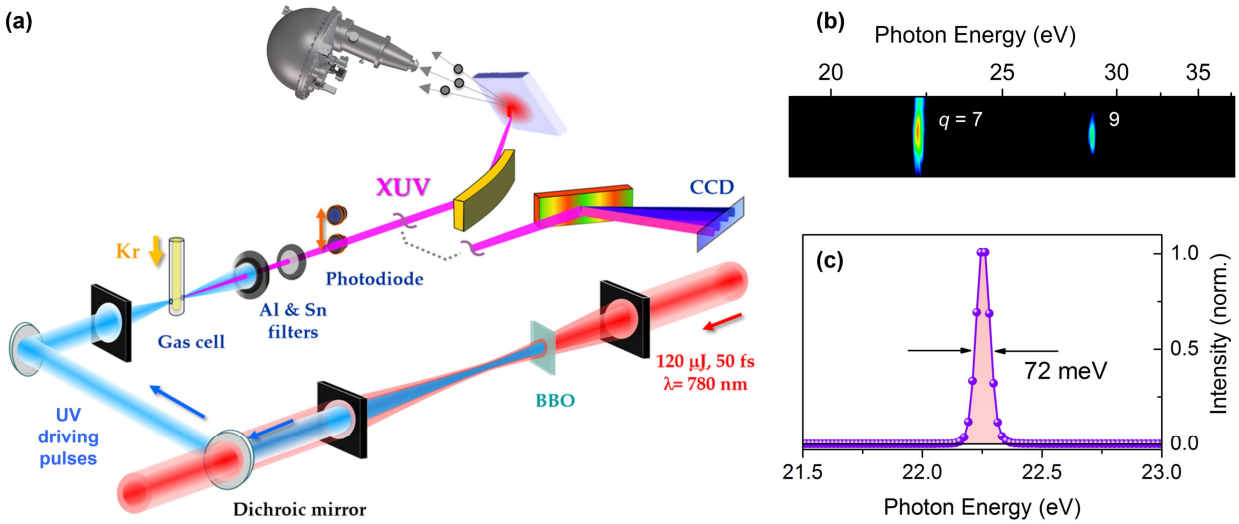

Figure 1. (a) Bright source of extreme-UV (XUV) femtosecond pulses at 50-kHz repetition rate for time-resolved photoemission spectroscopy. (b) CCD image of the XUV spectrum, showing the $q = 7^{th}$ and 9^{th} harmonics of the 390 nm ultraviolet driving pulses. (c) Close-up of the narrowband spectrum of the 7^{th} harmonic used to probe the dynamics in the time-resolved ARPES experiments.

which necessitates intense laser fields around 10^{14} W/cm^2 to drive strong-field ionization, electron acceleration, and recombination in atomic gases [11]. Since phase-matching is critical for efficient HHG, the process is typically driven by energetic mJ-scale pulses at low repetition rates, which can be loosely focused to optimize the phase-matching conditions [12]. In contrast, efficient HHG at high repetition rates of ≈50 kHz and beyond – with typically μJ-level driving pulses – is challenging, due to the difficulty of achieving phase-matching in the resulting tight laser focus. Previous approaches include direct XUV generation with limited conversion efficiency [13-15], or intra-cavity HHG at multi-MHz repetition rates which boosts the XUV power but is unsuited for pump-probe studies with strong excitation [16]. Novel driving sources have also been applied to boost the HHG power, including Yb solid-state amplifiers, fiber amplifiers, and optical parametric chirped-pulse amplifiers [17, 18]. A powerful approach to boost the conversion efficiency results from wavelength scaling of the HHG atomic dipole, as previously evidenced in schemes using mJ pulses loosely focused at lower repetition rates [19]. In this context, we have recently explored the feasibility of UV-driven HHG in the tight-focusing regime, establishing a highly-efficient 50-kHz source of narrowband XUV pulses optimally suited for trARPES [10].

Our scheme, outlined in Fig. 1(a), thus employs a cascaded approach consisting of second harmonic generation followed by HHG in Kr gas. At the outset, a cryo-cooled Ti:sapphire regenerative amplifier (KMLabs Wyvern 500) supplies near-IR femtosecond pulses with ≈11 Watt average power and 50-kHz repetition rate. After splitting off a fraction for the pump beam, pulses with 120-μJ energy are focused onto a 0.5-mm thick BBO crystal for frequency doubling with 40% efficiency. For this, loose focusing with a 1-m focal length lens avoids nonlinear ionization in air. The resulting UV pulses around 390 nm exhibit a 3-nm bandwidth and ≈48 μJ pulse energy. To generate high harmonics, the femtosecond UV pulses are collimated, separated from the near-IR via dichroic mirrors, and then sharply focused onto a gas cell in vacuum to a ≈20 μm spot (>10^{14} W/cm^2 peak intensity). The gas cell is constructed of an end-sealed glass capillary with 1-mm inner diameter, positioned perpendicular to the beam and using laser-drilled entrance and exit holes.

With this approach, we observe the emission of strong XUV harmonics. For this, the XUV is separated from the driving beam with a thin Al filter, and then propagates towards the ARPES chamber or alternatively into a grating-based spectrometer. As shown in Fig. 1(b), the spectrum measured on a CCD exhibits bright peaks around 22.3 eV and 28.6 eV that correspond, respectively, to the 7^{th} and 9^{th} odd harmonics of the UV driving pulses. For the brightest harmonic around 22.3 eV, the photon flux reaches 3.3×10^{13} photons/s at the source point which corresponds to a high conversion efficiency of 5×10^{-5}. This large HHG efficiency represents a two-orders-of-magnitude increase over driving directly with the near-IR laser output. The enhancement arises from the combined effects of dipole wavelength scaling and improved phase-matching due to reduced Guoy-phase effects and a higher ionization tolerance [10].

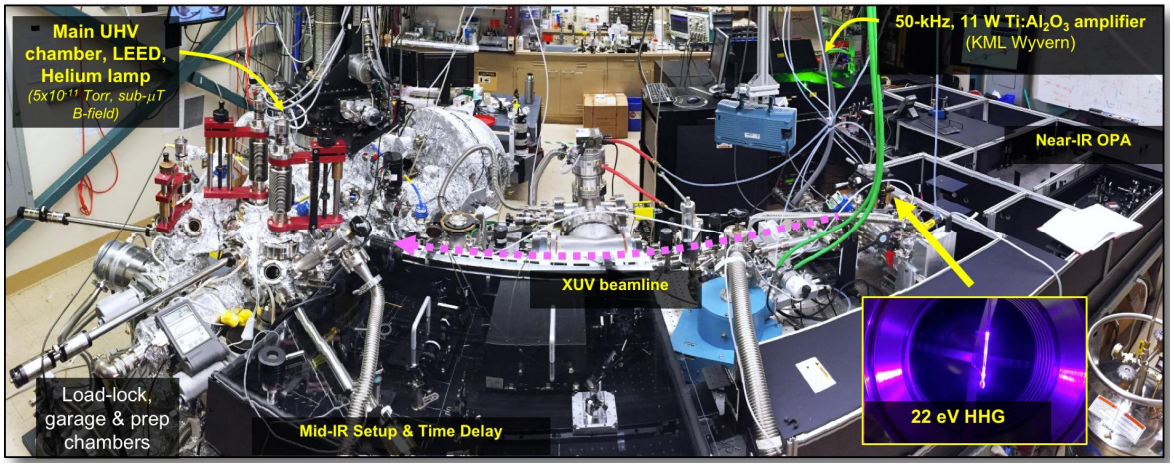

Figure 2. Picture of the time-resolved ARPES setup utilizing a 50-kHz femtosecond XUV source, with main sections as indicated. Inset: picture of the Kr gas cell used for high harmonic generation, which is housed within a vacuum chamber and consists of an end-sealed glass capillary. The bright glow stems from the ionized Kr atoms.

Importantly, the XUV harmonics are narrow with 72 meV width at 22.3 eV as shown in Fig. 1(c). Moreover, the UV-driven HHG also entails a large harmonic separation of ≈6.4 eV, allowing for isolation of individual harmonics using thin metal filters instead of a complex monochromator. We achieve high-contrast isolation of the 22.3 eV harmonic via the combination of thin Sn and Al filters. Our XUV harmonics source thus optimally combines several key parameters important for trARPES, including a high flux, narrow bandwidth, direct isolation, and high repetition rate at photon energies beyond 20 eV that enables sensitive studies with full momentum access in many two-dimensional and layered materials.

For the trARPES experiments, we have integrated this source into a complex photoelectron spectroscopy setup as indicated in Fig. 2. After the HHG chamber, the XUV beam traverses an Al filter and is then focused and steered onto the sample using a gold-coated toroidal mirror and an additional second Au-coated flat mirror controlled by piezo-actuators. The moderate 6 mrad divergence of the XUV beam is well suited for this beamline setup. Several molecular turbo pumps guarantee a differential pumping scheme along the ultrahigh vacuum (UHV) beamline, which together with the Sn filter situated before the main ARPES chamber results in a UHV sample environment with pressures around 5×10^{-11} Torr. The XUV flux at the sample after filtering is around 10^{10}-10^{11} ph/s which enables rapid acquisition.

The pump beam is coupled in close to the main ARPES chamber and is sent onto the sample nearly parallel to the XUV beam. As customary, a mechanical delay stage allows for scanning of the time delays and covers an overall temporal scanning window of 1.5 ns. The main ARPES chamber is equipped with a hemispherical electron detector (Scienta R4000) to map the emitted photoelectrons in momentum and energy along a given slice in *k*-space. The whole chamber contains a double μ-metal shield to reduce the magnetic field around the sample. Moreover, a six-axis manipulator and cryostat is employed to provide flexible access to the various photoemission angles and to temperatures down to $T = 12$ K. Three additional chambers are attached, which provide for sample loading into the UHV, for long term storage of the samples at UHV conditions, and for sample preparation.

3. TIME-RESOLVED PHOTOEMISSION IN $MOSE_2$

In first applications of our trARPES setup, we have investigated lamellar transition-metal dichalcogenides, including the dynamics in the charge-density wave compound $TiSe_2$ and both bulk and monolayers of semiconducting $MoSe_2$. In the following we will discuss measurements of bulk $MoSe_2$, which was grown by chemical vapor deposition and exhibits a low *n*-type background carrier density of $n_D \approx 2\times10^{16}cm^{-3}$ as determined by THz spectroscopy.

For the trARPES measurements, the crystal was mounted on a sample puck, and transported onto the six-axis manipulator in the main chamber. We cleaved the sample (with the help of a top-mounted ceramic post) in-situ at pressures $<5x10^{-11}$ Torr and at cryogenic temperature ($T = 80$ K) to achieve a clean surface for the photoemission

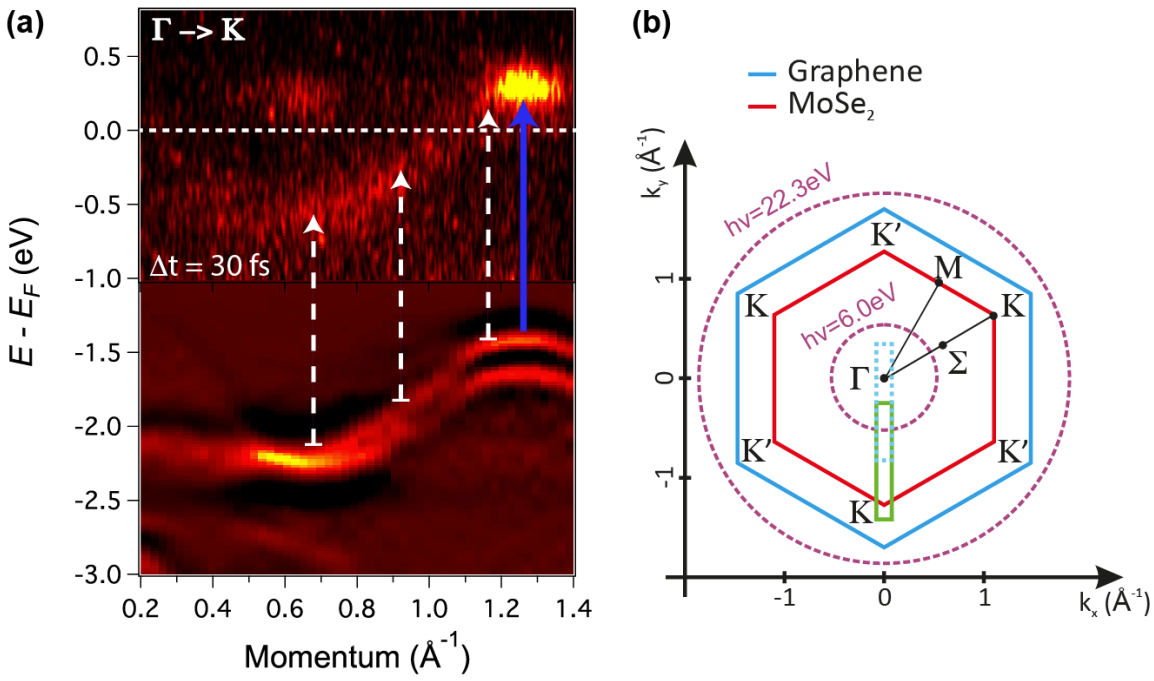

Figure 3. (a) Equilibrium ARPES map (lower part) of the valence band in the high symmetry Γ-K-direction, as determined from the second-derivative of the ARPES signals. Upper part: photoexcited carriers at the local conduction band minimum around K, at Δt=30fs after pumping with 1.58 eV (blue arrow). White arrows: illustration of LAPE shift as discussed in the text. (b) Accessible in-plane momentum space of graphene and $MoSe_2$, comparing the use of 6 eV and 22.3 eV photons. We consider a maximum emission angle of 60° in line with typical experimental limits. Dashed blue and solid green boxes: momentum range for the ARPES signals in Figs. 3a and 4, for a tilt angle of 12º and 27º respectively.

studies. Before conducting time-resolved measurements, the equilibrium band structure was characterized using the XUV pulses as shown at the bottom of Fig. 3(a). This exploits the XUV photon energy that provides access to the full in-plane Brillouin zone and easily reaches the *K*-Point of $MoSe_2$. This advantage is further illustrated in Fig. 3(b), which compares the momentum range accessible with 6 eV and 22.3 eV photons within the in-plane Brillouin zone of graphene and $MoSe_2$. The maximum emission angle considered here is 60°, which presents a reasonable limit for most trARPES experiments. The green box in Fig. 3(b) indicates the momentum range along the high symmetry Γ-K direction, as transmitted through the analyzer slit and measured for the data in Fig. 3(a). In this case, the sample inclination is 27° with respect to the normal.

In the time-resolved ARPES studies, the sample was photo-excited with 1.58 eV near-IR pump pulses resonant to the direct optical transition around the *K*-Point. The electronic response was then probed with the time-delayed XUV pulses. The upper part in Fig. 3(a) displays the non-equilibrium response at Δt = 30 fs after excitation, indicating a strong signal appearing around the *K*-point. As derived from additional measurements (not shown) the K-point signal decays while the quasi-particles scatter on a 70-fs time scale towards the global minimum of the conduction band at the Σ-point. This corresponds to rapid inter-valley scattering in $MoSe_2$, in concordance with recent studies of other TMDCs [20-22].

It should be noted that the feature of the photo-excited signals in Fig. 3(a) which resembles the valence band structure is an artifact that appears around time-zero due to the laser-assisted photoelectric effect (LAPE). This effect, which was first discovered in helium and later observed in solids [23, 24], corresponds to a "dressing" of the photo-emitted electrons by the intense laser field. This results in the absorption or emission of photons by the photoelectrons, leading to the appearance of the LAPE replica separated from the original bands by the pump photon energy (dashed lines in Fig. 3a). Moreover, the LAPE signals can be employed to estimate the temporal resolution which in our setup is ≈65 fs.

Figure 4 shows the non-equilibrium ARPES signals in a range that covers both the Γ and Σ points. As discussed above, inter-valley scattering leads to a build-up of the carrier distribution around the Σ-point in momentum space. This

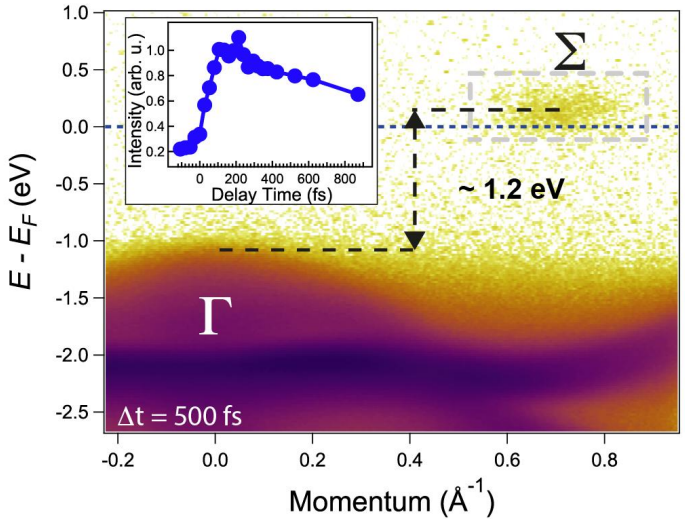

Figure 4. Time-resolved ARPES map along Γ–Σ at Δt = 500 fs pump-probe delay. The inset shows the time evolution of the non-equilibrium electronic signal around the Σ-point, with the integration range indicated by the dashed gray box.

dynamics is plotted in the inset of Fig. 4, corresponding to the signals integrated within the area inside the dashed gray box i.e. the electrons accumulating at the bottom of the conduction band. This renders the inter-valley scattering dynamics clearly visible, with the electronic response around Σ reaching its maximum about 100 fs after photo-excitation. Importantly, since the top of the valence band is located at the Γ-point and electron distribution at the Σ-point is the lowest energy level of the conduction band for all possible momenta, our trARPES data offer the possibility to directly measure the indirect gap in this material which we estimate to be E_g = 1.2eV ± 0.1 eV. Finally, we note that further analysis of the non-equilibrium dynamics exhibits intriguing signatures connected to the Coulomb interaction of the photo-excited carriers, which will be discussed elsewhere.

4. CONCLUSIONS

We have discussed a novel setup for time-resolved ARPES at high repetition rates based on a bright source of femtosecond and narrowband XUV pulses. This capability enables experiments that probe layered and two-dimensional materials with full access to the in-plane momentum space and with high sensitivity. In first experiments, we employed XUV trARPES to study the fundamental non-equilibrium carrier dynamics in layered transition-metal dichalcogenides. In layered $MoSe_2$, after resonant excitation around the direct K-point gap we observe rapid quasi-particle scattering towards the conduction band minimum at the Σ-point. Moreover, the indirect gap of this material can be determined by mapping the transient signals from otherwise unoccupied conduction band states. The powerful combination of a narrowband, high repetition-rate, and high flux XUV source with ARPES thus opens new possibilities for studies of quantum materials to sensitively track their non-equilibrium quasi-particles and band structure dynamics across momentum space.

5. ACKNOWLEDGEMENTS

We thank Hyejin Ryu, Yi-De Chuang, and Jonathan Denlinger for helpful discussions, as well as Sef Tongay and Junqiao Wu for providing high quality dichalcogenide samples. Ultrafast studies were supported by the US Department of Energy, Office of Basic Energy Sciences (DOE BES), Division of Materials Sciences and Engineering under contract DE-AC02-05CH11231, carried out within the Ultrafast Materials Science program at Lawrence Berkeley National Laboratory. J.H.B. gratefully acknowledges a fellowship from the German Science Foundation (DFG).

REFERENCES

[1] J. Graf, C. Jozwiak, C. L. Smallwood *et al.*, "Nodal quasiparticle meltdown in ultrahigh-resolution pump–probe angle-resolved photoemission," Nature Physics, 7(10), 805-809 (2011).

[2] J. D. Rameau, S. Freutel, A. F. Kemper *et al.*, "Energy dissipation from a correlated system driven out of equilibrium," Nature Communications, 7, 13761 (2016).

[3] T. Rohwer, S. Hellmann, M. Wiesenmayer *et al.*, "Collapse of long-range charge order tracked by time-resolved photoemission at high momenta," Nature, 471(7339), 490-3 (2011).

[4] J. A. Sobota, S. L. Yang, A. F. Kemper *et al.*, "Direct optical coupling to an unoccupied dirac surface state in the topological insulator Bi_2Se_3," Physical Review Letters, 111(13), 136802 (2013).

[5] Y. H. Wang, H. Steinberg, P. Jarillo-Herrero *et al.*, "Observation of Floquet-Bloch states on the surface of a topological insulator," Science, 342(6157), 453-7 (2013).

[6] K. F. Mak, C. Lee, J. Hone *et al.*, "Atomically thin MoS_2: a new direct-gap semiconductor," Physical Review Letters, 105(13), 136805 (2010).

[7] K. S. Novoselov, A. Mishchenko, A. Carvalho *et al.*, "2D materials and van der Waals heterostructures," Science, 353(6298), 9439 (2016).

[8] Y. Ye, Z. J. Wong, X. Lu *et al.*, "Monolayer excitonic laser," Nature Photonics, 9(11), 733-737 (2015).

[9] S. B. Desai, S. R. Madhvapathy, A. B. Sachid *et al.*, "MoS_2 transistors with 1-nanometer gate lengths," Science, 354(6308), 99-102 (2016).

[10] H. Wang, Y. Xu, S. Ulonska *et al.*, "Bright high-repetition-rate source of narrowband extreme-ultraviolet harmonics beyond 22 eV," Natue Communications, 6, 7459 (2015).

[11] T. Popmintchev, M.-C. Chen, P. Arpin *et al.*, "The attosecond nonlinear optics of bright coherent X-ray generation," Nature Photonics, 4, 822-832 (2010).

[12] E. Constant, D. Garzella, P. Breger *et al.*, "Optimizing high harmonic generation in absorbing gases: Model and experiment," Physical Review Letters, 82, 1668-1671 (1999).

[13] F. Lindner, W. Stremme, M. Schätzel *et al.*, "High-order harmonic generation at a repetition rate of 100 kHz," Physical Review A, 68(1), 013814 (2003).

[14] M.-C. Chen, M. R. Gerrity, S. Backus *et al.*, "Spatially coherent, phase matched, high-order harmonic EUV beams at 50 kHz," Optics Express, 17, 17376-17383 (2009).

[15] C. M. Heyl, J. Güdde, A. L'Huillier *et al.*, "High-order harmonic generation with μJ laser pulses at high repetition rates," Journal of Physics B: Atomic, Molecular and Optical Physics, 45(7), 074020 (2012).

[16] J. Lee, D. R. Carlson, and R. J. Jones, "Optimizing intracavity high harmonic generation for XUV fs frequency combs," Optics Express, 23, 23315 (2011).

[17] S. Hädrich, A. Klenke, J. Rothhardt *et al.*, "High photon flux table-top coherent extreme-ultraviolet source," Nature Photonics, 8(10), 779-783 (2014).

[18] M. Puppin, Y. Deng, O. Prochnow *et al.*, "500 kHz OPCPA delivering tunable sub-20 fs pulses with 15 W average power based on an all-ytterbium laser," Optics Express, 23(2), 1491-7 (2015).

[19] E. L. Falcão-Filho, C.-J. Lai, K.-H. Hong *et al.*, "Scaling of high-order harmonic efficiencies with visible wavelength drivers: A route to efficient extreme ultraviolet sources," Applied Physics Letters, 97, 061107 (2010).

[20] R. Bertoni, C. W. Nicholson, L. Waldecker *et al.*, "Generation and Evolution of Spin, Valley, and Layer-Polarized Excited Carriers in Inversion-Symmetric WSe_2," Physical Review Letters, 117(27), 277201 (2016).

[21] P. Hein, A. Stange, K. Hanff *et al.*, "Momentum-resolved hot electron dynamics at the 2H−MoS_2 surface," Physical Review B, 94(20), 205406 (2016).

[22] R. Wallauer, J. Reimann, N. Armbrust *et al.*, "Intervalley scattering in MoS_2 imaged by two-photon photoemission with a high-harmonic probe," Applied Physics Letters, 109(16), 162102 (2016).

[23] T. E. Glover, R. W. Schoenlein, A. H. Chin *et al.*, "Observation of laser assisted photoelectric effect and femtosecond high order harmonic radiation," Physical Review Letters, 76(14), 2468-2471 (1996).

[24] L. Miaja-Avila, C. Lei, M. Aeschlimann *et al.*, "Laser-assisted photoelectric effect from surfaces," Physical Review Letters, 97(11), 113604 (2006).